CIVIL ENGINEERING JOURNAL

Article no. 14

THE CIVIL ENGINEERING JOURNAL 2-2025

USE OF CONTACTLESS SPATIAL DATA COLLECTION METHODS FOR SNOW COVER MONITORING: CASE STUDIES FROM CZECH MOUNTAINS

Jan Pacina, Ondřej Soukup, Dominik Brétt, Petr Novák and Jan Popelka

J. E. Purkyne University, Faculty of Environment, Department of Geoinformatics, Ústí nad Labem, Pasteurova 1, Czech Republic; jan.pacina@ujep.cz

ABSTRACT

Accurate documentation of snow cover is critical for hydrological modeling, climate adaptation planning, and risk assessment in mountainous regions. This study presents a comprehensive methodology for snow cover monitoring using UAV-based LiDAR scanning, tailored to the specific environmental and technical constraints of Central European mountain ranges. Field campaigns were conducted across several Czech border mountain locations (Ore Mountains, Giant Mountains, Beskids Mountains), utilizing DJI Matrice 300 RTK equipped with Zenmuse L1 or L2 LiDAR sensors. Due to limitations in deploying traditional ground control points (GCPs) in remote and protected areas, the methodology emphasizes reliance on GNSS RTK corrections and minimal GCP use. The influence of two GNSS reference networks (CZEPOS and TopNet) was evaluated through photogrammetric analysis, revealing systematic elevation biases and spatial autocorrelation, with TopNet yielding slightly better results.

Various point cloud post-processing workflows were tested, including smoothing and noise filtering in DJI Terra, TerraSolid, and CloudCompare. The best visual and statistical results were obtained using a combined approach supplemented by a single foldable GCP. Ground point classification methods were assessed in both snow-free and snow-covered conditions. The most reliable method for snow-free filtering was the Spatix-based algorithm in TerraSolid, while snow-covered scenes required custom multi-criteria filtering in CloudCompare.

Validation was performed using over 4,500 RTK GNSS ground points and manual snow probe measurements. The methodology proved robust despite uncertainties from vegetation interference and manual measurement limits. This study delivers practical guidelines for operational snow cover documentation under constrained field conditions, and proposes improvements for future automation and validation.

KEYWORDS

UAV LiDAR, Snow cover, GNSS RTK, Point cloud processing, Bare ground filtering, Mountain environments

INTRODUCTION

Modeling snow cover is essential for understanding the dynamics of the hydrological cycle [1], managing water resources, and predicting the impacts of climate change [2]. Snow serves as a significant reservoir of water, influencing runoff in watersheds [3], water availability during dry seasons [4], and overall ecological stability [5]. Accurate snow cover models enable us to estimate the amount of water stored in snow (known as snow water equivalent, SWE) and provide critical data for water resource management [6], particularly in regions where snow is the primary source of water for populations and agriculture [7]. Another key reason for modeling snow cover is monitoring the impacts of climate change [8], [9]. In warmer regions or seasons, the snowline is shifting, the total volume of snow is decreasing, and snowmelt is occurring earlier, affecting both ecological and

socioeconomic systems [10]. Models based on accurate snow cover data help scientists and policymakers understand these changes in the landscape and facilitate better planning for adaptation to new climate conditions [11].

Beyond environmental and hydrological applications, snow cover modeling is also crucial for winter sports [12], transportation [13], and energy production [14]. In mountainous areas, models can optimize infrastructure maintenance and safety measures [15]. Wind and hydroelectric power facilities can use snow cover models to improve energy management [16]. Precise information about snow cover and its dynamics is critical for a wide range of applications, from local to global scales [17].

Snow cover can be measured using various methods. Manual methods are traditional approaches to snow measurement that require direct physical presence in the field. The simplest method is to use a snow gauge rod or measuring rod, where the depth of the snow cover is measured on site [18]. This method is undemanding in terms of equipment, but time-consuming and dependent on the availability of the measured locations [19]. More detailed snow analysis is made possible by measuring snow profiles, where a profile is dug in the snow layer and its structure, density and temperature are evaluated. This information is crucial for avalanche risk prediction or hydrological modelling, but the method requires expertise and careful implementation in the field [20].

With the growing need for more accurate data and frequent monitoring of snow cover, automated methods have become popular. Among the most widespread are ultrasonic snow gauges, which measure the distance between the sensor and the snow surface using ultrasonic waves [21]. This method allows for continuous measurements and is commonly installed at weather stations.

Remote sensing and photogrammetry allow monitoring of snow cover over large areas using various sensors located on satellites, aircraft or UAVs. Aerial and ground-based LiDAR (Light Detection and Ranging) allows detailed measurements of changes over time [22], while SAR radar systems (e.g. Sentinel-1) provide information on snow cover even in cloudy conditions [23].

Optical images from satellites such as Landsat or Sentinel-2 allow mapping of the presence of snow and its spectral properties, but their accuracy is lower than that of radar methods. UAV photogrammetry provides detailed models of snow cover by comparing images before and after snowfall, while historical photos can in some cases be used to reconstruct the evolution of snow conditions in the past. Another option is to use sensors in the field, such as temperature and humidity sensors, which provide indirect information about the properties of the snow. For comprehensive analysis, data from these methods are often combined with numerical models that allow simulation of snow accumulation and melting based on meteorological data, remote sensing and other input parameters.

In the following text, we will focus mainly on the documentation of snow cover using LiDAR data. Laser scanning (LiDAR) and point cloud analysis have revolutionized the accuracy of snow cover modeling. These technologies allow for detailed mapping of the Earth's surface both before and after snowfall, enabling precise quantification of snow layer thickness. The high spatial resolution of LiDAR captures fine-scale variations in snow cover, which is crucial for studying local microclimatic conditions and their influence on snow melting or accumulation. The results of such modeling are not only valuable for hydrological applications but also for mitigating risks such as avalanches or extreme flooding caused by rapid snowmelt.

The use of LiDAR scanners in combination with UAVs allows for fast, cheap and operative documentation of snow cover even in hard-to-reach areas. Our research presented in this paper is focused on verifying the possibilities of using mobile laser scanning in combination with UAVs in our national conditions (Czech Republic, Europe), especially focusing on data quality and accuracy. When working in remote mountainous and difficult-to-reach areas, we are limited by the quality of the GNSS RTK solution, the very limited ability to deploy control points and the problematic validation of the obtained data. The aim of the presented research is to define possible qualitative parameters of the resulting snow cover data, methodological recommendations for their processing and the presented validation of the results in the field with application in the border mountains of the Czech

Republic, as the snow data was collected and processed as part of a research project of the Technology Agency of the Czech Republic called „Analysis of spatio-temporal dynamics of snow cover for the purposes of prediction and prevention of hydrological extremes and dimensioning of adaptation measures within land consolidation“ (TA CR SNOW).

MATHERIALS AND METHODS

The TA CR SNOW project was solved for a total of 3 years (2022 – 2024). During the individual years of the project, there was a gradual improvement of the surveying technology and thus changes in the methodology of data collection. With regard to the very warm winters in the monitored period in Central Europe, activities aimed at monitoring the snow cover were directed to the border areas of the Czech Republic – the Ore Mountains, the Giant Mountains and the Beskids Mountains.

Areas of interest

The area for testing the accuracy of individual methods and verifying the methodology of data collection and processing was chosen in the Ore Mountains – the ridge part at an altitude of about 900 m above sea level (see Figure 1). This area was chosen with regard to the existence of previous ground measurements, the combination of open spaces (mountain meadows) and forest, proximity to the state border (most of the snow monitoring within the TA CR SNOW project was carried out in border areas), which brings aspects such as poor mobile signal coverage and possible problematic RTK solutions, the possibility of using UAVs without permission. Within the localities in the Ore Mountains, the Giant Mountains and the Beskids Mountains, data collection and processing were carried out on the basis of the methodology presented in the following text. However, due to the inaccessibility of many sites in the Giant Mountains and Beskids Mountains during winter, extensive validation measurements could not be performed there. Therefore, detailed accuracy analysis is presented only for the Ore Mountains, while field campaigns in the other regions helped to confirm the general applicability of the methodology and identify potential limitations. The data processed within the area of Giant Mountains and the Beskids Mountains are thus not presented within this paper.

Fig. 1 - Area of interest

Hardware and software used for data acquisition and processing

The data collection was carried out by a DJI Matrice 300 RTK drone (carrier), which is a UAV (Unmanned Aerial Vehicle) suitable for mapping. It can carry multiple sensors and is equipped with a device to receive real-time GNSS RTK corrections. In the course of our research, we used the DJI Zenmuse P1 (full-frame camera), DJI Zenmuse L1, and DJI Zenmuse L2 LiDAR sensors.

The following software tools were used for data processing: DJI Terra Pro – raw LiDAR data processing, TerraSolid and CloudCompare – LiDAR data postprocessing, ArcGIS Pro – LiDAR data processing, visualization and analysis, Agisoft Metashape – image data processing from the DJI P1 sensor.

The point clouds are exported in DJI Terra in the ETRS89 UTM 33N coordinate system, while the exact NTv2 grid transformation to the Czech national coordinate system S-JTSK (EPSG 5514) is not possible in this software. External software using the certified transformation key was used for transformation to EPSG 5514.

GNSS correction networks

A total of two GNSS reference networks were used for field data collection. The CZEPOS network provides correction data for GNSS measurements in real time with high accuracy. According to testing carried out by the Land Survey Office and Cadastral Offices on 150 trigonometric points in 25 locations throughout the Czech Republic, the following mean errors were achieved for RTK services: horizontal accuracy (m_{xy}): 1–2 cm and vertical accuracy (m_h): 2–3 cm [24]. The TopNet network works with similar accuracies [25]. However, it is important to note that accuracy may be affected by distance from the reference station and current environmental conditions. In general, accuracy can decrease as the distance from the reference station increases. The RTK method states a horizontal accuracy of approximately 10 - 20 mm + 1 ppm (part per million), which means 1 mm for every kilometer of distance from the reference station. Vertical accuracy tends to be slightly lower. Thus, at a distance of 10 km from the reference station, the horizontal error would be approximately 10 mm (basic error) + 10 mm (1 mm/km × 10 km) = 20 mm. There are studies that suggest that RTK accuracy does not decrease significantly with distances up to 80 km from the reference station

[26],[27]. However, further publications confirm the dependence of accuracy on the distance from the reference station [26],[28].

Data collection methodology

The methodology of data collection assumes that snow cover data are measured in mountainous, hard-to-reach locations. It is necessary to transport equipment with a total weight of 52.4 kg (drone, battery, sensor, means of transport) to the selected location. Most of the Czech border mountains are included in large-scale protected areas (Protected Landscape Areas, National Parks). Access to the sites (especially during winter) is difficult and in most cases, it is not possible to use motor vehicles. Movement within a given locality is in many cases, with regard to the rugged terrain, the amount of snow, the wintering grounds of the game, impossible or even forbidden. The presented methodology of data collection and processing thus reflects the possible shortcomings that we may encounter when collecting data in such conditions.

Fig. 2 A and B - drone transportation in the mountainous area; C - DJI Matrice 300 RTK equipped with Zenmuse L2 LiDAR scanner

For the analysis of snow cover, it is necessary to process data from two-time horizons (landscape with snow and without snow). For data collection, we had the opportunity to try a number of different sensors and approaches - classic photogrammetry, aerial laser scanning and laser scanning where a drone was used as a carrier.

All these methods have one common weak point – the very problematic or impossible placement of ground control points (GCPs) within the site of interest, which make the collection of LiDAR data more accurate. GCP for LiDAR scanning must be large and provided with a high-quality reflective layer. At a flight altitude of 100 m AGL, the recommended size of the edge of a square GCP is 70 – 80 cm [30]. The 6 GCP set can thus weigh well over 10 kg. These bulky and heavy GCPs are difficult to transport to remote locations when moving on foot, or it is problematic to deploy these GCPs within the site at all. Mountainous areas are in most cases forested and therefore the precise targeting of GCP centers using GNSS is problematic. As part of the presented methodology, we will focus on evaluating the quality of the data obtained only with the help of RTK solutions on a drone. At the Lesná test site, the use of the so-called folding GCP was verified, which was located at the launch site and the center coordinates were measured with RTK GNSS. In the Results chapter, the effect of the application of the detected "corrections" from this one GCP on the entire resulting point cloud will be tested.

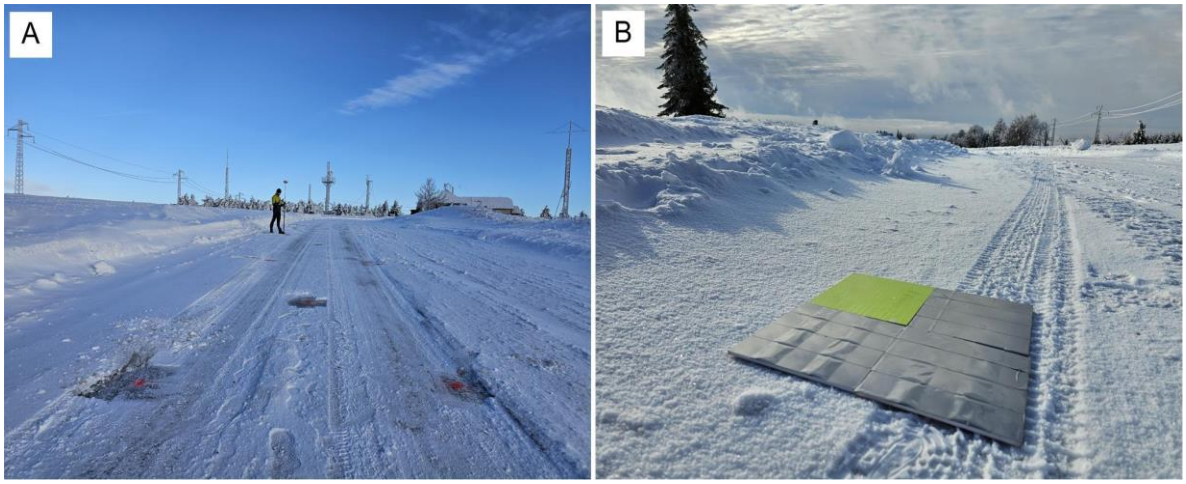

Fig. 3 A - measurement of control points on the road; B - foldable Ground Control Point with different reflective materials

Before starting the actual data collection, it is necessary to select a suitable sensor. Within the TA CR SNOW project, data collection was carried out using both a photogrammetric sensor (DJI P1) and LiDAR sensors. With regard to the character of the landscape (forested areas), photogrammetry seems to be an unsuitable method in most cases. Since it is very difficult (if at all) to model (snowy) terrain under trees in densely overgrown terrain.

The actual preparation for the flight is no different from the preparation for a normal flight - it is only necessary to ensure that the batteries for the drone are warm at all times. The flight was always planned from a height of 100 m AGL, with the Terrain Follow function activated, which ensures that the drone's flight altitude follows changes in the topography of the terrain. When taking test images with the DJI P1 sensor, at an altitude of 100 m AGL, the resulting resolution of the acquired image data is 0.88 cm/pixel. However, photogrammetric snow cover photography requires a specific approach according to [30] it is advisable to shoot in low sunlight (the relief is better rendered on snow) and the camera needs to be set to take underexposed images (ideally in RAW format for possible post-processing). When using the DJI Zenmuse L1 sensor, 3 reflections of the laser beam were set, while the DJI Zenmuse L2 sensor had 5 reflections. The resulting density of the point cloud is approximately 530 points/m^2 from DJI L1 and 600 points/m^2 from DJI L2.

We rely on GNSS correction data for our own data collection. It receives the drone in real time via the RTK service. RTK correction data available within public (mostly commercial) reference networks are dependent on the coverage of the area by the mobile signal, which is needed for real-time data transmissions. During our measurements, we had access to two reference networks – the national Czepos network and the commercial TopNet network. Having active access to two reference networks proved to be practical in case there was a problem with finding an RTK solution and fixing the position with cm accuracy when using the (preferred) Czepos network.

The correction data of our flights has always been received through the so-called virtual reference station, which should be located automatically within the scanned location, while the corrections are derived from the surrounding reference stations. Experience has shown that it is advisable to manually disconnect the drone from the reference network before the start of the mission and then connect it again – this will in many cases correct the position of the virtual reference station to the data collection point.

Data processing methodology

A suitable way of data processing is crucial to obtaining the quality data needed to create an accurate snow cover model. Photogrammetric images, which contain coordinates of the center of the image and values of Yaw, Pitch and Roll in EXIF, were processed in a standard way in the Agisoft

Metashape SW environment. Data derived from photogrammetric images (DSM, point clouds) are not suitable for modeling snow cover in areas covered by forest. We mention this method here only for the complexity of the methodology, and in the following text we will focus mainly on LiDAR data processing.

The raw data from the DJI L1 and DJI L2 sensors needs to be processed in the native DJI Terra program as part of the first step. For data processing in our research, we used the DJI Terra Pro program, which is a paid version of the DJI Terra tool. One of the main differences between the "free" version and the paid "Pro" version is the ability to use the Optimize Point Cloud function to process data from the LiDAR sensor. According to information from the DJI website [31], this function is suitable for removing noise, improving point alignment, smoothing out dense clouds, correcting errors caused by drone movement. The research did not identify an expert study that would verify the effect of this function on the resulting point cloud. However, according to discussions within DJI community groups, user experiences suggest that this feature makes sense and leads to an increase in the quality of the resulting point cloud. In our research, we focused on empirically verifying the influence of this function on the resulting data.

However, DJI Terra Pro only processes the raw data, performs point cloud optimization, and exports the LAS file for the area of interest. Further processing takes place in TerraSolid SW, where we perform further filtering/smoothing.

The last step in data processing is the removal of noise (so-called isolated points), which can still be identified in the data even after applying the optimization functions in the DJI Terra Pro and TerraSolid environments. Here we use the CloudCompare software and the Statistical Outlier Removal function (SOR).

Another problematic aspect that affects the quality of the resulting data is point filtering. To analyze snow cover, we need so-called "bare ground" data. There are many software tools that allow this – we will focus on the possibilities of filtering "ground" points in the TerraSolid, CloudCompare and ArcGIS Pro environments. Each of these software products contains different algorithms for filtering points, the influence of which on data quality will be verified.

Methodology for verifying the quality of measurement

In our research, we used two reference networks (Czepos, TopNet), the accuracy of which is defined by tests carried out by network operators (see the previous text). Verification of the use of the reference network in combination with UAVs was analyzed, for example in [32]. In our case, we wanted to verify the accuracy of our two reference networks. For this purpose, test photogrammetric imaging was carried out at an open site. Within this locality, 7 GCPs were deployed, where these points will be used to evaluate differences in coordinates [X, Y, Z]. In addition, 75 control points in the field were surveyed, which will be used to verify the Z coordinate. All points were surveyed by RTK GNSS – the resulting coordinate is the result of an average of 20 observations at the point. Claimed accuracy m_{xy} = 1 cm, m_h = 1 – 2 cm. The entire site was then covered with photogrammetric images from two flights – the first using the Czepos reference network, the second using the TopNet network (consequent flights). The data were photogrammetrically processed in the Agisoft Metashape environment. The coordinates [X, Y, Z] were read on the derived data (orthophoto, DSM) and compared with the directly measured data. The analysis of the differences of individual coordinates allows us to see the differences in the accuracies of individual reference networks. In the DJI Terra environment, it is possible to find the coordinates of the virtual reference station in the "Base center point settings" settings to verify that the virtual reference station has been placed in a suitable position.

Verification of the quality of LiDAR data was carried out at the Lesná test site (see Fig. 1). A total of 46 points on the surface of the road that passes through the area of interest were marked here (see Fig. 3-A). These points were again surveyed using RTK GNSS (20 observations at each point), the points were measured repeatedly after about 2 hours. The resulting coordinates of the points are then the average of these two measurements. The stated accuracy of the measured control points is m_{xy} = 1 cm, m_h = 1 – 2 cm. However, only the Z coordinate is evaluated to evaluate

the quality of LiDAR data. X and Y coordinates cannot be verified on this type of signalling. As part of the scanning in January 2025, experimental "folding" GCPs were deployed within the site of interest (see Fig. 3-B). Using them, we are able to perform a basic evaluation of the effect of the presence of a low number of GCPs on the resulting point cloud.

In order to determine the influence of individual approaches to smoothing and optimization of the point cloud during its processing, the processed point cloud was evaluated within the defined asphalt road - always visually and in comparison, with the surveyed points. We tested the effect of incremental optimization using the features implemented in DJI Terra Pro, Terra Solid, and Cloud Compare (see Figure 7). The optimization method that produces the most accurate and smoothest data was then used for all processed datasets, which are evaluated within other criteria.

Another factor that affects the accuracy of the resulting cloud is the "bare ground" filtering method. Here, we tested different approaches implemented in TerraSolid, ArcGIS Pro and CloudCompare. Control points (more than 4500) were surveyed by RTK GNSS technology within the entire test site. With regard to the number of points, individual points were measured using 5 observations.

In January 2025, laser scanning was also supplemented with validation measurements with a snow probe (see Fig. 4). Using this data, we will try to validate the data processed according to the created methodology.

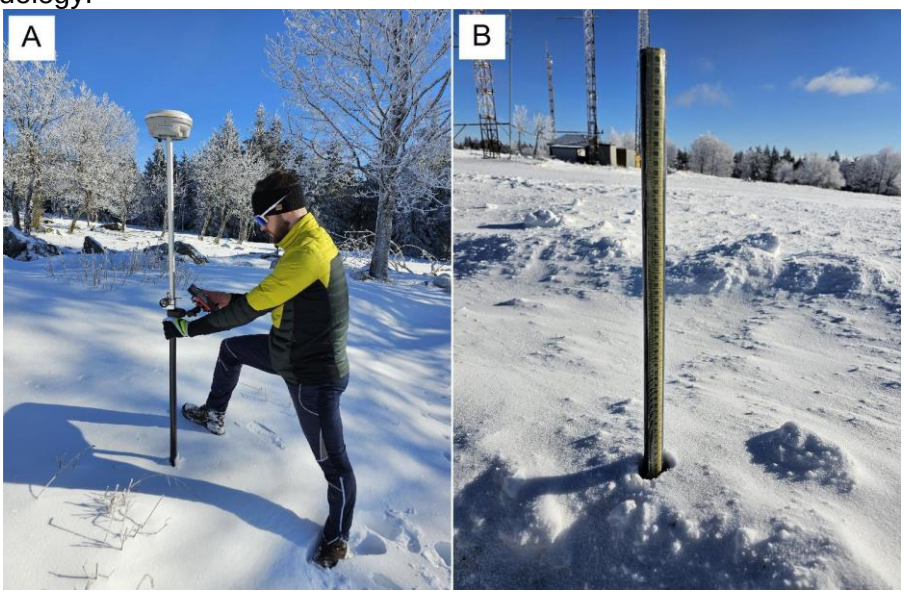

Fig. 4 - Snow probe verification measurements

Statistical methods

Geostatistical methods applied to differences in coordinates were used to evaluate the quality of individual datasets. Three main quality aspects of model errors (i.e., differences between modelled and reference coordinates) were evaluated [33]:

1. Model errors should not be spatially autocorrelated, meaning they should be randomly distributed in space. To evaluate this aspect, the Global Moran's Index was calculated. The statistical significance of the index was evaluated based on the p-value derived from a normally distributed z-score. The analysis was conducted using the *Spatial Autocorrelation (Global Moran's I)* tool in ArcGIS Pro (version 3.2.0).
2. Model errors should be normally or at least symmetrically distributed, with a central tendency close to zero**.** The Jarque–Bera test was used to assess the univariate normality of the errors. In addition, standardized skewness and standardized kurtosis were computed to examine

the shape of error distribution. Basic descriptive statistics including the mean, median, standard deviation, and RMSE were also calculated to characterize the accuracy and variability of the modelled data. All computations were carried out using PAST software (version 4.16c).

3. There should be no significant dependency between model errors and altitude. For this purpose, the Pearson correlation coefficient was calculated to assess potential linear relationships. The coefficient also allows for straightforward significance testing. The analysis was performed in PAST software (version 4.16c).

RESULTS

Within this chapter, the results of the presented methodology for the collection and validation of snow cover data will be evaluated. With regard to the detailed geostatistical analysis of the processed data, other tables and graphs are available in Appendix.

Reference Networks

As introduced in the chapter Data and methods - during the measurement we used a total of two GNSS RTK reference networks - national Czepos and commercial TopNet. The aim of the comparison is to obtain an objective overview of the accuracy of individual GNSS reference networks during measurements carried out under the same conditions: at the same time, at the same location and under the same satellite configuration. Within the selected area, 7 points were signaled that were surveyed (and will be used to evaluate X, Y and Z coordinates) and 75 points measured without signalling, which were used only for the evaluation of the quality of the Z coordinate. This area was then photogrammetrically scanned using a drone and a DJI P1 camera in two aerial missions (using different reference networks). The data were then photogrammetrically processed into orthophoto and digital surface model. Details on measurement, data collection and processing are given in the Data and methods chapter.

Differences in X, Y and Z coordinates were then used for the accuracy analysis. An example of measured coordinates and coordinates derived from orthophoto (location of points within a signaled control point) is shown at Fig. 5.

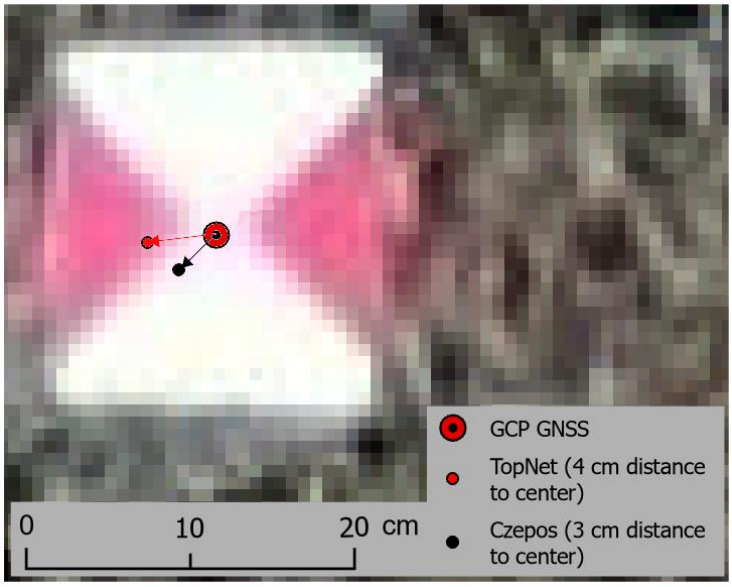

Fig. 5 - Positional differences of Ground Control Point center derived from photogrammetric processing using different GNSS correction networks.

Within the framework of a detailed geostatistical analysis (according to the methodology presented above), 3 qualitative aspects were evaluated. A detailed statistical evaluation, including tables and graphs, is available in Appendix.

According to the Moran indexes and its p-values (Appendix Table 1), spatial autocorrelation is statistically significant in both models, but in different components. While the TopNet network shows significant autocorrelation in the X coordinate, the spatial structure of the Czepos network is more pronounced in the Y axis. The remaining components do not show spatial clustering of errors and can be considered randomly distributed.

The normality condition was explored using skewness and kurtosis and subsequently tested by the Jarque–Bera test. In all cases, no significant deviations from the normal distribution were found (p-values > 0.1).

Pearson correlation coefficients between errors and altitude show a very strong linear dependence in all cases, with the highest correlation recorded in the Y coordinate for both networks.

The results of our qualitative test confirmed the announced accuracies of the reference networks (with regard to the influence of the distance from the reference station), even though the centers of the control points are shifted by a distance of 3 cm in the case of the Czepos network and 4 cm in the case of the TopNet network.

Both reference networks exhibit statistically significant positive vertical biases, with Czepos showing slightly larger systematic errors and RMSE compared to TopNet. Although TopNet performs marginally better in terms of overall accuracy, both datasets are affected by significant spatial autocorrelation and non-normal error distributions. The observed weak negative correlation with elevation suggests a minor trend toward increasing underestimation of height at higher elevations

Concerning the Z coordinate accuracy - both Czepos and TopNet reference networks show a statistically significant positive bias in elevation, with TopNet demonstrating slightly better overall accuracy and stability (lower RMSE and standard deviation). The spatial distribution of errors is non-random, exhibiting strong spatial autocorrelation in both systems. Error distributions are non-normal, negatively skewed, and slightly leptokurtic, indicating a majority of values slightly below the mean and the presence of a few large positive outliers. Additionally, a weak negative correlation between error and altitude suggests a minor tendency to underestimate elevations at higher altitudes. Overall, while both systems introduce systematic elevation overestimation, TopNet provides marginally more

precise and consistent results, making it the preferable option for height data acquisition in this context.

Influence of post-processing operations on LiDAR data

As mentioned in the methodological part of the article, when processing LiDAR data, we verified the influence of standard and less standard post-processing tools on the quality of the resulting data. For this purpose, 46 points were signaled and coordinates measured with RTK GNSS within the area of interest (see Fig. 3-A), which are used for qualitative evaluation of the output data. Given the overlap of individual datasets, it is possible that a lower number of control points were used in some accuracy analyses.

From the information available in DJI Terra Pro, the positions of the virtual reference stations that were used for GNSS corrections within individual data collection campaigns were visualized. As can be seen in Fig. 6-A, the 2 centers of the virtual stations are shifted by about 15 km from the scanning area. These are datasets obtained 6/2023 and 12/2023.

Furthermore, we tested the effect of using one folding GCP with dimensions of 40 x 40 cm on increasing the quality of the processed point cloud. As can be seen in Fig. 6-B, the center of the GCP identified in the processed cloud is shifted by about 15 cm from its real position surveyed by GNSS.

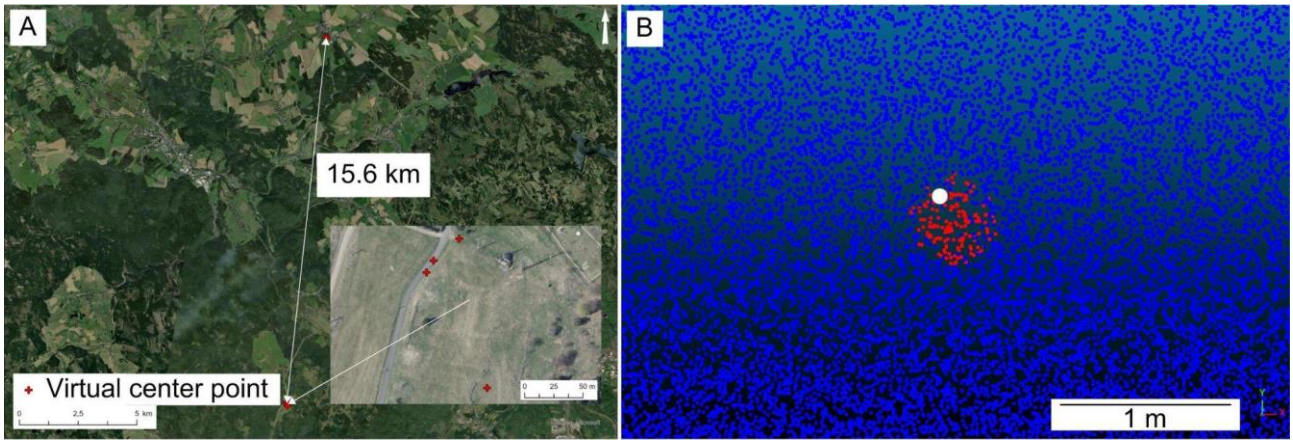

Fig. 6 A - Virtual GNSS correction stations centers; B - Ground Control Point (red square) identified based on the LiDAR intensity and the GNSS measured center (white point).

The results of the applied post processing approaches were evaluated visually and using statistical analyses of Z-coordinate differences on 46 control points within the processed datasets. The RMSE indicator was used for each step (see Figure 7) and a detailed geostatistical evaluation was then used for the best performing approach.

Raw data entering the post processing are presented in Figure 7-A (Smooth 1). In the first step, smoothing (point cloud optimalization) in DJI Terra Pro (Figure 7-B; Smooth 2), smoothing in TerraSolid (Figure 7-C; Smooth 3), smoothing in DJI Terra Pro and then in TerraSolid (Figure 7-D; Smooth 4) were applied to the data. A SOR filter was then applied to the data from Figure 7-D (Smooth 4) in the CloudCompare environment (Figure 7-E; Smooth 5). Detailed description of the applied filters is given in Appendix – Table 3.

According to the evaluation of the RMSE results, the best data set is based on Figure 7-C - data that was smoothed only by the function in TerraSolid. However, based on visual evaluation, the data to which the smoothing filters have been applied in DJI Terra Pro, TerraSolid and the Cloud Compare SOR filter come out best. In order to thoroughly verify the quality of data filtration, a detailed statistical evaluation of the data from 6/2023 presented on Figure 7-C and E was performed. Furthermore, the same approach was applied to the dataset from January 24, 2025. This dataset was chosen with regard to the use of an experimental folding control point. Quality evaluation was

carried out also on the derived point cloud, manually shifted by the detected correction vector in the sense of the center shift of the identified center of the control point and its measured position (see Fig. 6-B).

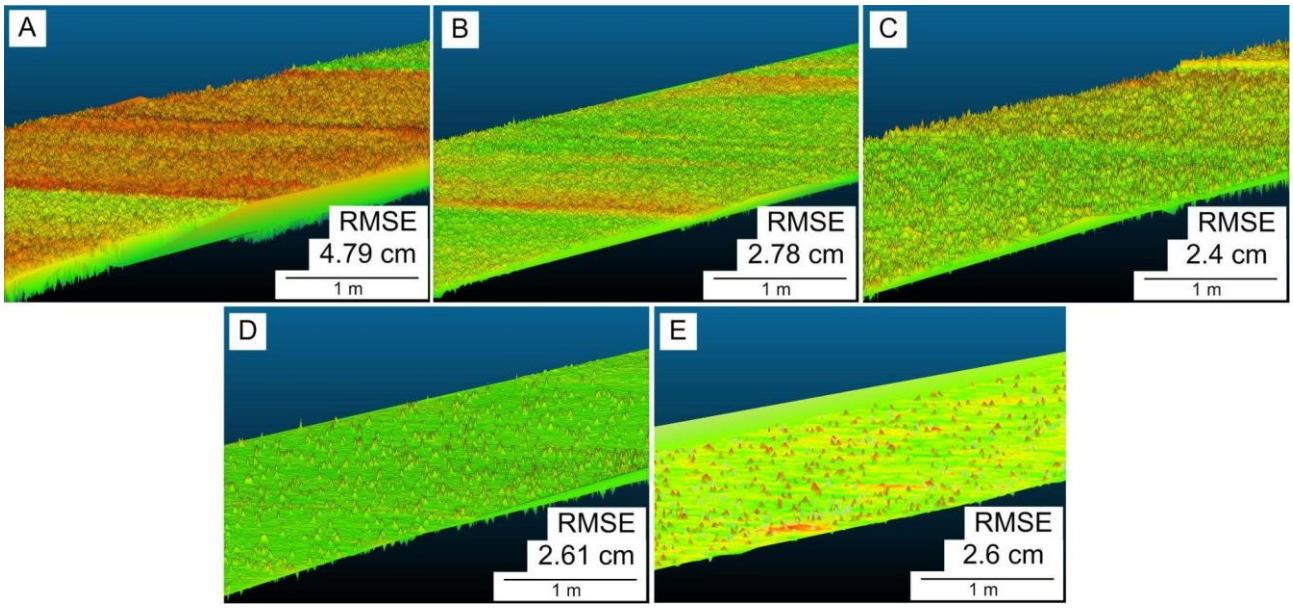

Figure 7 Results of application of methods for post-processing of LiDAR data. A - input data (without optimization); B - smoothing (point cloud optimalization) in DJI Terra Pro. C - smoothing in TerraSolid; D – point cloud optimalization in DJI Terra Pro and then smoothing in TerraSolid; E – data from D with Statistical Outlier Removal function applied.

Statistical evaluation of postprocessing operations

The differences found in the Z coordinate were subjected to a geostatistical analysis according to defined criteria. A detailed analysis of the results, including tables and graphs, is in Appendix (Figure 4, Table 4, Table 5, Figure 6).

The spatial autocorrelation of model errors was statistically significant for both smoothing methods (Smooth 3 and Smooth 5), which confirms the significant spatial clustering of the errors. The central tendency was negligible – the average and median of the Smooth 3 were zero, the Smooth 5 slightly above zero. Both methods achieved low dispersion with RMSE below 3 cm (0.024 m and 0.026 m), with a narrow, symmetrical distribution and no outliers. Normality tests showed no significant deviations from the normal distribution. Visual and quantitative analysis showed that the application of smoothing algorithms significantly improves accuracy compared to the unsmoothed model (RMSE 4.79 cm). The Smooth 3 and Smooth 5 methods show the best results, with Smooth 3 having the advantage of completely symmetrical error distribution and lower variability, making it the most balanced choice. Methods with DJI Terra optimization achieved fewer outliers, but slightly higher deviations due to the suppression of height details. The highest internal consistency is confirmed by the interquartile range (IQR) for Smooth 3, while outliers are more common for Smooth 1, 4 and 5. The Smooth 3 seems to be a suitable choice, especially where maintaining the height details of the surface is key. On the other hand, Figure 7-C shows that the Smooth 3 method still leaves the surface noisy. The Tab. 5 (in Appendix) clearly shows that the use of control points (even if only one) significantly increases the quality of the cloud. The Smooth 5 method supplemented by moving the cloud to the control point was therefore used for further data processing.

The impact of "bare earth" filtering on data quality

Within the framework of continuous experimental testing of the accuracy of the obtained data, it was shown that with regard to the ruggedness of the terrain of the area of interest (pits, ditches, stone walls but as well high grass), the method of filtering the cloud to the "bare ground" has an impact on the resulting structure of the point cloud. Points classified as ground are important for deriving a summer data set ("snow-free" data. For this purpose, several algorithms for filtering "bare ground" points were tested, which are contained in software products that are available for research and that are commonly used - TerraSolid (Spatix), CloudCompare and ArcGIS Pro (Clasif1 – TerraSolid (Spatix)-based workflow with additional height-from-ground classification and SOR filtering in CloudCompare; Clasif2 – ArcGIS Pro Standard Classification combined with SOR filtering; Clasif3 – ArcGIS Pro Conservative Classification and SOR filtering; Clasif4 – ArcGIS Pro Aggressive Classification and SOR filtering; Clasif5 – TerraSolid (Spatix) Classify Ground function with custom terrain settings (e.g., max building size, terrain angle); Clasif6 – Same as Clasif5 with additional SOR filtering in CloudCompare; Clasif7 – Pure CloudCompare-based classification using SOR filter and CSF (Cloth Simulation Filtering) plugin with Relief method. Detailed description of the filtering methods is presented in Appendix – Table 6.

The quality assessment was based on more than 4,500 RTK GNSS points and 46 road-marked points used to verify the impact of filtering algorithms on point cloud smoothing. The analysis was conducted using three qualitative parameters. All methods showed significant spatial autocorrelation of errors (Moran's I between 0.107 and 0.180; $p < 0.01$), indicating a clustered spatial structure. The error distribution deviated from normality (Jarque-Bera test $p < 0.01$), with pronounced kurtosis (kurtosis > 20) and negative skewness; the most extreme characteristics were observed for the "Clasif 7" variant (kurtosis = 67.9; skewness = -4.664). This variant also exhibited the highest negative central tendency and RMSE (0.301 m). The lowest RMSE values were observed for the "Clasif 1" and "Clasif 5" variants (0.247 m and 0.250 m, respectively). A high correlation ($r > 0.99$) was found between the "Clasif 2–4" methods, while "Clasif 7" correlated minimally with the others ($r < 0.1$), indicating its fundamentally different character. Most methods yielded comparable results, except for "Clasif 7," which showed the greatest variance and deviations. The best balance of accuracy, stability, and consistency was performed by the "Clasif 1 Spatix" method, which achieved the lowest RMSE, low variability, and strong correlation with other variants.

However, when these filters were applied to snow-covered landscapes, they caused a significant removal of point cloud data representing the snow surface. For the purpose of isolating snow cover from LiDAR data, a combination of filters was applied in CloudCompare, based on point height above terrain, surface roughness, point density, and normal orientation. Height above ground was used as a basic criterion to separate the snow layer from taller vegetation, while the calculation of surface roughness in a small window helped distinguish the smooth snow surface from the irregular structure of vegetation. Tree branches were further identified using their differing slope—points with deviating surface normals were detected and subsequently removed. Point density can also used to eliminate sparse structures typical of branches. By combining these criteria within CloudCompare's visualization environment, vegetation was effectively suppressed while maintaining a continuous (dense) snow cover point cloud. The detailed filtering procedure is provided in the Appendix – section "Methodology for filtering "bare ground" with snow cover".

Measurement with a snow gauge stick, map of snow cover thickness and other possible approaches

Validation of the measured data using a snow probe was carried out during two monitoring campaigns in January 2025. During the LiDAR scanning on January 13, 2025, a total of 43 test points were measured, and on January 24, 2025, 42 points were surveyed. Prior to the second data collection, a thaw followed by new snowfall occurred—this caused the lower snow layers to refreeze, introducing uncertainty as to whether the snow probe reached the actual ground surface. Therefore, these data were excluded from the accuracy evaluation. The point was first surveyed using RTK GNSS and then with snow probe. The resulting map is shown on Fig. 8. Snow depths measured

with a snow pole are represented by points. The used (winter) point cloud (January 13, 2025) was also shifted based on the differences found on the folding GCP.

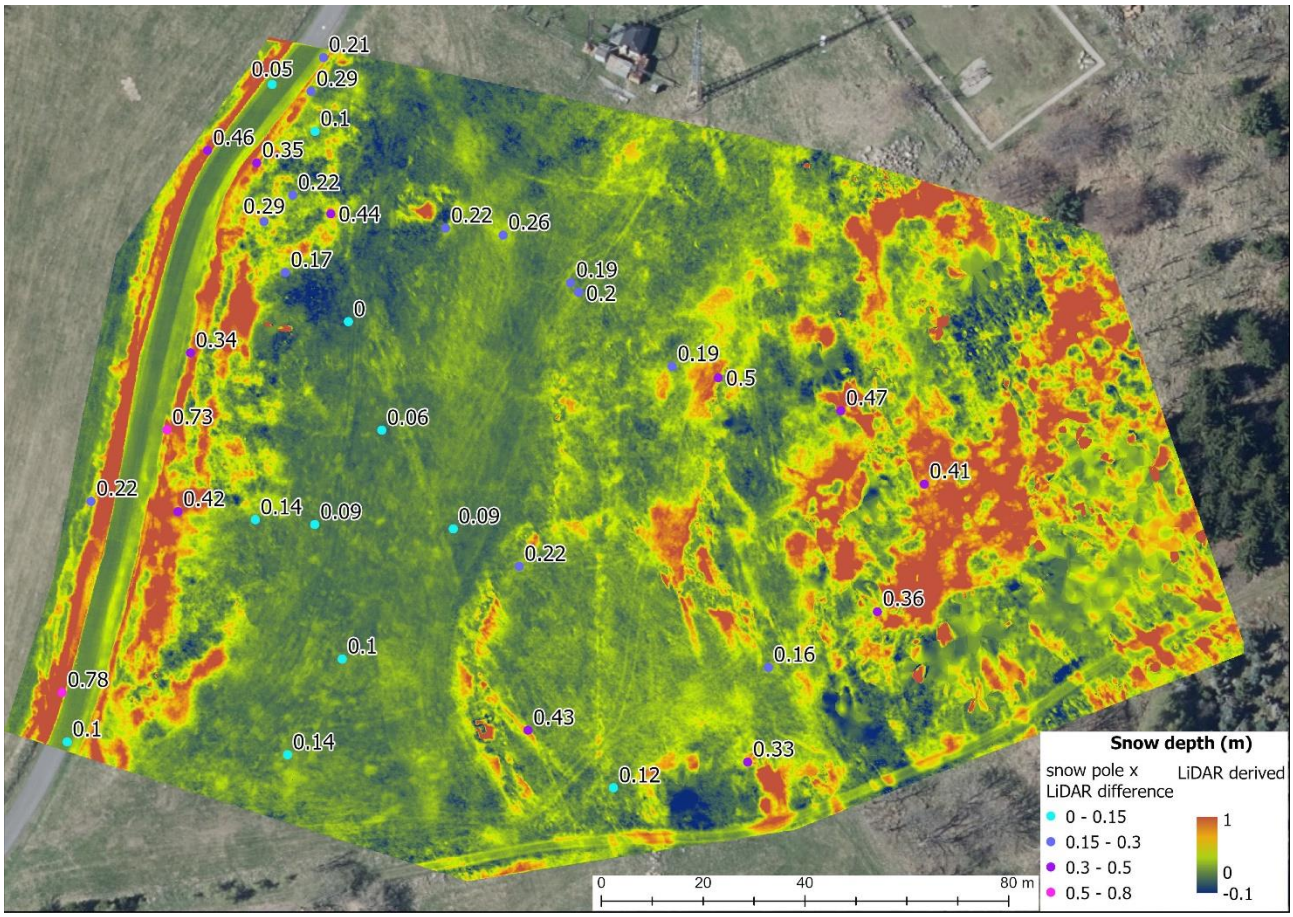

Fig. 8 - Snow depth map including snow depth measurements using the snow pole

DISCUSSION

Our comparative analysis of the Czepos and TopNet GNSS correction networks revealed subtle but systematic differences in positional accuracy. While both networks fulfilled the expected precision requirements for UAV-based RTK measurements, TopNet demonstrated slightly lower RMSE and standard deviation in elevation data, as well as a lower level of spatial autocorrelation in the X-Y plane. This is consistent with findings by authors such as [33], who emphasize the importance of network density and real-time signal quality in mountainous terrain. Notably, both networks exhibited a consistent positive elevation bias of 8–11 cm, likely related to the virtual base station location, which was ~15 km from the area of interest in some campaigns. These biases are particularly important when no ground control points are available to compensate for such systematic errors.

Our tests showed that the application of smoothing algorithms significantly improves LiDAR data accuracy. The unsmoothed model (Smooth 1) had an RMSE of 4.79 cm, whereas all smoothed variants reduced errors to approximately 2.5 cm. Among them, Smooth 3 (TerraSolid only) provided the most balanced results, with zero mean and median error, and symmetrical distribution of residuals. However, visual analysis revealed that the Smooth 5 method (a combination of DJI Terra, TerraSolid, and CloudCompare SOR) yielded the most aesthetically consistent and least noisy surface. This highlights an important trade-off: numerical indicators such as RMSE may not fully

capture the surface smoothness or visual interpretability, which are often critical in hydrological or environmental applications.

An important methodological insight is that UAV LiDAR campaigns without ground control points are feasible, but subject to cumulative vertical errors. Our analysis shows that even a single foldable GCP, if accurately positioned using RTK GNSS, can significantly improve vertical alignment when used as a co-registration anchor for the point cloud. Moreover, point cloud smoothing in DJI Terra Pro appears to slightly overestimate elevation values, as shown by consistent positive shifts in error distributions. For this reason, we recommend using TerraSolid-based smoothing followed by intensity and geometry-based filtering, especially in areas where no GCPs can be deployed.

Ground classification algorithms proved useful not only for identifying terrain but also for suppressing noise in the point cloud. However, in snow-covered landscapes, standard bare-ground filters tended to mistakenly classify snow surfaces as terrain, particularly in open meadows. Our custom filtering method based on CloudCompare allowed for more accurate separation of snow from vegetation by combining height above ground, surface roughness, return number, and normal orientation. This multi-criteria approach proved essential for isolating snow cover in complex forest–meadow mosaics.

Snow depth estimation from LiDAR requires precise subtraction of snow-free and snow-covered surfaces. However, the variability in vegetation height, especially in summer datasets, complicates this process. Tall grass tufts and uneven ground structures often remain partially unfiltered, resulting in false negatives (i.e., negative snow depth). We recommend collecting snow-free data during late autumn or after frost events when vegetation is flattened and less influential on terrain modeling. Although meteorological and logistical constraints may limit such campaigns, their added value in reducing ground surface uncertainty is considerable.

While snow probes remain a useful tool for in-situ snow depth validation, our study identified several uncertainties. First, GNSS survey poles used to define terrain elevation may penetrate deeply into soil or vegetation, producing biased ground values. Second, snow probes may not reliably indicate the true base of the snowpack, especially after thaw-refreeze events that form ice layers or cause probe deflection. These factors limit the reliability of manual measurements as validation for LiDAR-derived snow thickness. Future field campaigns may benefit from integrated sensor probes or repeated time-series observations to reduce ambiguity.

The outcomes of this study go beyond methodological refinement and have direct implications for applied environmental monitoring. The presented UAV-based LiDAR workflow offers a scalable and replicable approach to snow documentation in mountainous regions with limited ground access. Regional water authorities, environmental protection agencies, and land-use planners may benefit from the spatially explicit data generated through this approach. In particular, accurate snow thickness mapping supports improved hydrological modeling, flood risk estimation, and planning of adaptation strategies in response to climate change. Moreover, the ability to document snowpack variability across open and forested terrain can inform conservation management in protected areas, such as national parks or nature reserves, where ground-based sensors are often infeasible. Although the study area covers 3.1 hectares, it encompasses a representative range of terrain variability and snow depths (0–1 m). This diversity, combined with the availability of historical ground measurements, makes it a suitable site for detailed methodological validation. Data obtained through this methodology are already being applied in hydrological studies to assess snow water equivalent (SWE) and related flood risks. Additional results, including analyses of SWE measurements performed in the Beskids Mountains, will be published separately.

The current methodology involves multiple software environments and manual processing steps, including point cloud filtering, noise removal, classification, and validation. While each step ensures high-quality outputs, the process remains time-intensive and requires significant operator expertise. Future work should explore the integration of automated workflows using open-source libraries (e.g., PDAL, Open3D) or batch-processing tools in CloudCompare and TerraSolid. Such

developments could facilitate near-real-time snow monitoring over large areas and support operational deployment in remote sensing programs by governmental or academic institutions.

Operating UAVs in ecologically sensitive regions such as mountain ridges, forests, and protected landscape areas presents a range of logistical and ethical challenges. Our methodology was developed with careful attention to environmental regulations and conservation priorities. Equipment was transported manually to minimize disturbance, flight durations were kept minimal, and sensor deployments avoided critical habitats (e.g., wintering grounds of wildlife). These constraints, while challenging, underscore the importance of designing monitoring approaches that are both technologically effective and environmentally responsible. Future work should further investigate how UAV-based methods can be harmonized with nature protection policies to enable sustainable long-term monitoring.

CONCLUSION

This study presents a validated methodology for UAV-based LiDAR documentation of snow cover in the complex environmental conditions of Central European Mountain regions. The results highlight the importance of multiple technical and methodological factors that significantly influence the quality and usability of derived snow depth data.

First, the choice of GNSS correction network plays a measurable role in positional accuracy. While both tested networks (Czepos and TopNet) met expected standards, they exhibited systematic elevation biases and significant spatial autocorrelation. TopNet showed marginally better performance, particularly in elevation accuracy and error dispersion, making it a preferable choice for height-sensitive applications when ground control points are unavailable.

Second, the study demonstrates that point cloud post-processing has a critical effect on model quality. Among the tested approaches, the TerraSolid smoothing method (Smooth 3) provided the most balanced numerical results, while a more comprehensive workflow including DJI Terra, TerraSolid, and CloudCompare filtering (Smooth 5) yielded visually superior and less noisy outputs. When supported by a single ground control point, the quality of the resulting surface model improved significantly, confirming the utility of even limited GCP integration.

Third, the filtering of "bare ground" in snow-free datasets was shown to be a decisive step for the accurate estimation of snow depth. The Spatix-based filtering approach (Clasif 1) achieved the most stable results across more than 4,500 GNSS-validated points. In snow-covered scenes, standard ground classification algorithms often failed due to confusion between snow and vegetation. A combination of geometric criteria (e.g., roughness, normal orientation, and height above ground) in CloudCompare proved effective for isolating the snow surface while minimizing vegetation artifacts.

Finally, the study identified limitations in both the reference (snow-free) and validation (snow pole) data. Tall vegetation in summer months introduced negative snow depth values, suggesting that snow-free scanning is best conducted in late autumn or winter. Manual snow depth measurements also suffered from uncertainties related to ground contact and snowpack structure, underscoring the need for more robust in-situ validation techniques in future work.

Overall, this research contributes to the development of practical, field-tested workflows for high-resolution snow cover monitoring using UAV LiDAR systems. The proposed methodology is applicable in mountainous, remote, and protected landscapes, and offers valuable insights for hydrologists, environmental scientists, and land managers. Future research should aim to automate key processing steps, explore alternative validation methods, and extend the approach to different climatic zones and terrain types.

ACKNOWLEDGEMENTS

This research was supported by project TA ČR "Analysis of spatio-temporal dynamics of snow cover for the purposes of prediction and prevention of hydrological extremes and dimensioning of adaptation measures within land consolidation", reg. No. SS05010157.

REFERENCES

[1] Lizama, E., Somos-Valenzuela, M., Rivera, D., Lillo, M., Morales, B., Baraër, M., & Fernández, A. (2024). Role of mountain glaciers in the hydrological dynamics of headwater basins in the Wet Andes. Journal of Hydrology, 132413. doi:10.1016/j.jhydrol.2024.132413

[2] Sunita, N., Gupta, P. K., Gusain, H. S., Gill, A. S., & Sidhu, O. S. (2024). Snow Cover Variability in the Beas River Basin and its relation with climate parameters during 2007-2018. IOP Conference Series Earth and Environmental Science, 1326(1), 012147. doi:10.1088/1755-1315/1326/1/012147

[3] Schilling, S., Dietz, A., & Kuenzer, C. (2024). Snow Water Equivalent Monitoring—A Review of Large-Scale Remote Sensing Applications. Remote Sensing, 16(6), 1085. doi:10.3390/rs16061085

[4] Jenicek, M., & Ledvinka, O. (2020). Importance of snowmelt contribution to seasonal runoff and summer low flows in Czechia. Hydrology and Earth System Sciences, 24(7), 3475–3491.

[5] Slatyer, R. A., Umbers, K. D. L., & Arnold, P. A. (2024). Ecological responses to variation in seasonal snow cover. Conservation Biology, 38(2), e13727. doi:10.1111/cobl.13727

[6] Taheri, M., & Mohammadian, A. (2022). An Overview of Snow Water Equivalent: Methods, Challenges, and Future Outlook. Sustainability, 14(18). https://www.mdpi.com/2071-1050/14/18/11395

[7] Zha, H., Zhang, F., Tang, S., Zhang, L., & Luo, L. (2025). Unraveling the Distinct Roles of Snowmelt and Glacier-Melt on Agricultural Water Availability. AGU, 61(1). doi:10.1029/2023WR036898

[8] Poschlod, B., & Daloz, A. S. (2024). Snow depth in high-resolution regional climate model simulations over southern Germany – suitable for extremes and impact-related research? European Geosciences Union, 18(4). doi:10.5194/tc-18-1959-2024

[9] PAVELKA, Karel; ŠEDINA, Jaroslav a PAVELKA, Karel. Knud Rasmussen Glacier Status Analysis Based on Historical Data and Moving Detection Using RPAS. Online. *Applied Sciences*. 2021, roč. 11, č. 2. ISSN 2076-3417. Dostupné z: https://doi.org/10.3390/app11020754

[10] Wieder, W. R., Kennedy, D., Lehner, F., & Yamaguchi, R. (2022). Pervasive alterations to snow-dominated ecosystem functions under climate change. Proceedings of the National Academy of Sciences, 119(30). doi:10.1073/pnas.2202393119

[11] Lute, A. C., Abatzoglou, J., & Link, T. (2022). High-resolution snow model SnowClim: Dataset and applications for climate adaptation. Geoscientific Model Development, 15(13), 5045-5071. doi:10.5194/gmd-15-5045-2022

[12] Mitterwallner, V., Steinbauer, M., Mathes, G., & Walentowitz, A. (2024). Global reduction of snow cover in ski areas under climate change. PLOS ONE, 19(3). doi:10.1371/journal.pone.0299735

[13] Vionnet, V., Martin, E., Masson, V., Guyomarc'h, G., Naaim-Bouvet, F., Prokop, A., Durand, Y., & Lac, C. (2014). Simulation of wind-induced snow transport and sublimation in alpine terrain using a fully coupled snowpack/atmosphere model. The Cryosphere, 8(2). doi:10.5194/tc-8-395-2014

[14] Nousu, J. -P., Lafaysse, M., Mazzotti, G., Ala-aho, P., & Marttila, H. (2024). Modeling snowpack dynamics and surface energy budget in boreal and subarctic peatlands and forests. The Cryosphere, 18(1), 231–256. https://tc.copernicus.org/articles/18/231/2024/

[15] Abe, T., Iwasawa, S., Murakami, T., Ito, K., & Tomonori, U. (2019). Safety measures against snow and ice for safe and secure expressways. doi:10.1016/j.rse.2021.112345

[16] Soomro, S. -e-hyder, Soomro, A. R., Batool, S., & Guo, J. (2024). How does the climate change effect on hydropower potential, freshwater fisheries, and hydrological response of snow on water availability?, 14(65). doi:10.1007/s13201-023-02070-6

[17] Mott, R., Vionnet, V., & Grünewald, T. (2018). The Seasonal Snow Cover Dynamics: Review on Wind-Driven Coupling Processes. Cryospheric Sciences, 197(6). doi:10.3389/feart.2018.00197

[18] Proulx, H., Jacobs, J. M., & Burakowski, E. A. (2023). Brief communication: Comparison of in situ ephemeral snow depth measurements over a mixed-use temperate forest landscape. The Cryosphere, 17(8), 3435-3442. doi:10.5194/tc-17-3435-2023

[19] Mendoza, P. A., Musselman, K. N., & Revuelto, J. (2020). Interannual and Seasonal Variability of Snow Depth Scaling Behavior in a Subalpine Catchment. Advancing earth and space sciences, 56(7). doi:10.1029/2020WR027343

[20] Herla, F., Horton, S., Mair, P., & Haegeli, P. (2021). Snow profile alignment and similarity assessment for aggregating, clustering, and evaluating snowpack model output for avalanche forecasting. European Geosciences Union, 14(1), 239–258. doi:10.5194/gmd-14-239-2021
[21] Ryan, W. A., Doesken, N. J., & Fassnacht, S. R. (2008). Evaluation of Ultrasonic Snow Depth Sensors for U.S. Snow Measurements. Journal of Atmospheric and Oceanic Technology, 9(4), 1005–1015. doi:10.1175/2007JTECHA947.1
[22] Deems, J. S., Painter, T. H., & Finnegan, D. C. (2013). Lidar measurement of snow depth. Journal of Glaciology, 59(215), 467-479. doi:10.3189/2013JoG12J154
[23] Buchelt, S., Skov, K., Rasmussen, K. K., & Ullmann, T. (2022). Sentinel-1 time series for mapping snow cover depletion and timing of snowmelt in Arctic periglacial environments: case study from Zackenberg and Kobbefjord, Greenland. The Cryosphere, 2022(16), 625-646. doi:10.5194/tc-16-625-2022
[24] Postup testování přesnosti služeb a produktů CZEPOS. [Procedure for testing the accuracy of CZEPOS services and products] Czepos. Retrieved May 5, 2025, from https://czepos.cuzk.gov.cz/_postup.aspx
[25] GNSS positioning correction service. (2015). TopCon Positioning. Retrieved May 5, 2025, from https://www.topconpositioning.com/solutions/technology/infrastructure-software-and-services/topnet-live-corrections
[26] Gumilar, I., Bramanto, B., & Rahman, F. F. (2019). Variability and Performance of Short to Long-Range Single Baseline RTK GNSS Positioning in Indonesia. E3S Web of Conferences, 94(01012). doi:10.1051/e3sconf/20199401012
[27] Atiz, O. F., Konukseven, C., Ogutcu, S., & Alcay, S. (2022). Comparative analysis of the performance of Multi-GNSS RTK: A case study in Turkey. International Journal of Engineering and Geosciences, 2022(7), 67-80.
[28] Understanding RTK Accuracy and Its Dependence on Distance from the Base Station. Online. Point One Navigation. Dostupné z: https://support.pointonenav.com/understanding-rtk-accuracy-and-its-dependence-on-distance-from-the-base-station.
[29] BAYBURA, Tamer; TIRYAKIOĞLU, İbrahim a UĞUR, Mehmet Ali. Examining the Accuracy of Network RTK and Long Base RTK Methods with Repetitive Measurements. Journal of Sensors. 2019, roč. 2019.
[30] Ground Control Points- Tutorial. Online. Inflights. Dostupné z: https://help.inflights.com/en/articles/6495854-ground-control-points-tutorial.
[31] DJI Terra Release Notes. 4.5.0. 2025. Available from: https://terra-1-g.djicdn.com/263b7ee0f1fe477c91b7ca44348166fe/releasenotes/DJI%20Terra%20Release%20Notes.pdf.
[32] Martínez-Carricondo, P., Agüera-Vega, F., & Carvajal-Ramírez, F. (2023). Accuracy assessment of RTK/PPK UAV-photogrammetry projects using differential corrections from multiple GNSS fixed base stations. Geocarto International, 38(1). doi:10.1080/10106049.2023.2197507
[33] Pacina, J., Cajthaml, J., Kratochvílová, D., Popelka, J., Dvořák, V. & Janata, T. (2022). Pre-dam valley reconstruction based on archival spatial data sources: Methods, accuracy, and 3D printing possibilities. Transactions in GIS. 26(1), 385-420. ISSN 1361-1682. doi:10.1111/tgis.12854
[34] Schaefer, M. & PEARSON, A. (2021). Accuracy and precision of GNSS in the field. GPS and GNSS Technology in Geosciences. Vol. 2021, no. 19, pp. 393-414. doi:10.1016/B978-0-12-818617-6.00002-0